Received 16 July 2018; revised 21 September 2018 and 20 November 2018; accepted 9 December 2018. Date of publication 13 December 2018; date of current version 1 March 2019. The review of this paper was arranged by Editor C. Surya.

*Digital Object Identifier 10.1109/JEDS.2018.2886550*

# Symmetrical and Crossed Double-Sided Passivation Emitter and Surface Field Solar Cells for Bifacial Applications

**JYI-TSONG LIN [1] (Senior Member, IEEE), KON-YU HO[1], STEVE W. HAGA[2], AND WEN-HAO CHEN[1]**

1 Department of Electrical Engineering, National Sun Yat-sen University, Kaohsiung 80424, Taiwan
2 Department of Computer Science and Engineering, National Sun Yat-sen University, Kaohsiung 80424, Taiwan

CORRESPONDING AUTHOR: J.-T. LIN (e-mail: jtlin@ee.nsysu.edu.tw)

This work was supported by the Ministry of Science and Technology of Taiwan under Contact MOST-104-2221-E-110-029-MY3.

**ABSTRACT** This paper proposes symmetrical and crossed double-sided passivation emitter and surface field solar cells for bifacial applications which are fully compatible with the passivated emitter and rear contact (PERC) fabrication process. Our simulations use Silvaco TCAD Atlas, calibrated by real measurements. At an ideal albedo level where light enters both sides equally, these symmetrical and crossed structures boost energy by 88.78% and 106.74%, respectively. The reason for the crossed structure's better performance is that it has a surrounding electric field. The crossed structure also obtains a 40.18 mA/cm$^2$ short-circuit current ($J_{sc}$), a 0.67 V open-circuit voltage ($V_{oc}$), an 81.07% fill factor and a 21.93% conversion efficiency ($\eta$). Compared with PERC+, the crossed structure improves low bifaciality factor ($\varphi_\eta$) and increases $\eta$ by 6.44% and energy boost by 31.41% for bifacial. For more-realistic albedo levels, the structure also performs strongly. At the spectral albedo level of snow, the energy boost of the crossed structure is 102.06%, which is close to the performance at ideal albedo. At the spectral albedo level of white sand, the energy boost is 77.13%. At lower albedos, the energy boost remains between 20% and 30%.

**INDEX TERMS** Bifacial, silicon, PERC solar cells.

## I. INTRODUCTION

Recently, the conversion efficiency of silicon solar cells has approached a limit [1]–[3]. The conversion efficiency of monofacial solar cells is hard to improve further [4], [5]. To overcome this, power output can be boosted by using bifacial solar cells that can be irradiated by light from both the front and rear surfaces. Bifacial cells were demonstrated decades ago [6], but have only recently drawn wide interest.

One such cell is a bifacial passivated emitter and rear contact (PERC+). By placing a printed aluminum (Al) finger grid on the rear surface, the PERC+ cell allows light to enter the rear surface, where not blocked by the grid. Modern Al pastes allow the finger grid to maintain high conductivity [7]. PERC+ solar cells can be manufactured by the typical industry PERC process flow. This process is a mature technology with a high market share, which can reduce production costs [8].

Although the front surface on PERC+ cells can reach a power conversion efficiency of 21.6%, the rear-side efficiency is only 17.3% [9]. This mismatch significantly impacts overall efficiency, particularly in high albedo situations. This paper improves rear-side efficiency by placing emitters on both sides. We consider two options for this placement: symmetrical and crossed, as presented in Fig. 1. Their fabrication is fully compatible with the conventional PERC fabrication process.

These devices retain the excellent passivation and surface field of PERC solar cells. The crossed structure is found to have better the electron current density $J_{sc}$ and fill factor *F.F.*, because the emitter has a surrounding electric field that assists carrier transport. Moreover, since the emitter ratio is important for carrier transport [10] and the best performance is found by controlling the emitter ratio between the front and rear sides.

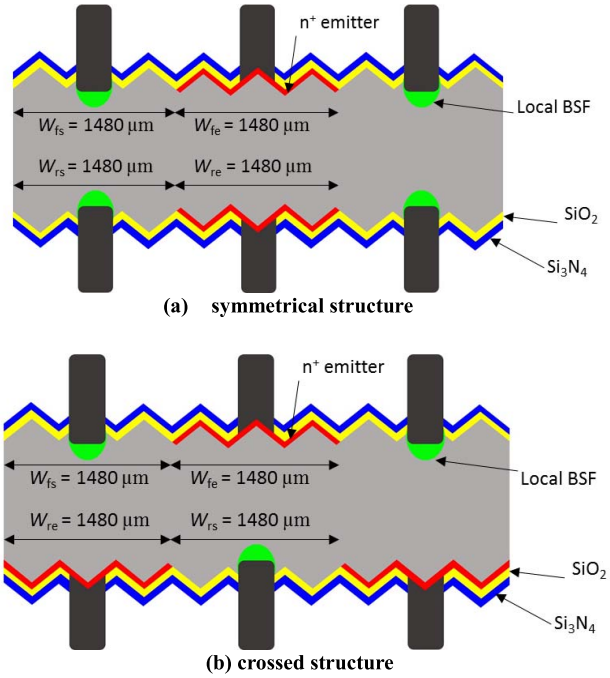


**FIGURE 1.** The schematic diagrams of our structures. (a) symmertrical double-sided emitters. (b) crossed double-sided emitters.

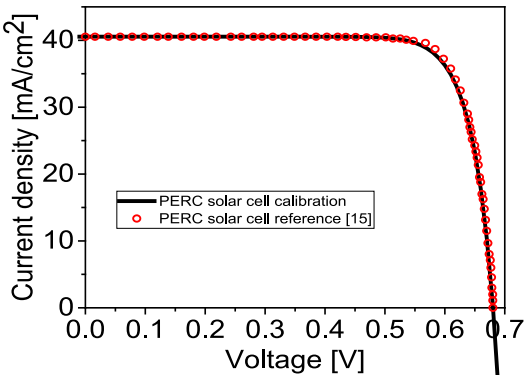


**FIGURE 2.** A comparison of the physically measured *I-V* curve of the PERC solar cell [15] and the calibrated simulation curve of that cell.

**TABLE 1.** Device parameters used in all our simulations. These parameters are calibrated from the real fabrication of a PERC cell [15].

| Parameter | $p^+$-c-Si | $n^+$-c-Si | p-c-Si |
|---|---|---|---|
| Layer Thickness (μm) | 5 | 1 | 170 |
| Energy Gap (eV) | 1.12 | 1.12 | 1.12 |
| Donor Doping Density ($cm^{-3}$) | NA | $1\times10^{20}$ | NA |
| Acceptor Doping Density ($cm^{-3}$) | $1\times10^{20}$ | NA | $1\times10^{15}$ |
| Electron Mobility ($cm^2/V_s$) | 1350 | 1350 | 1350 |
| Hole Mobility ($cm^2/V_s$) | 480 | 480 | 480 |
| Electron Life Time (μs) | 500 | 500 | 500 |
| Effective conduction band density ($cm^{-3}$) | $2.8\times10^{18}$ | $2.8\times10^{18}$ | $2.8\times10^{18}$ |
| Effective valence band density ($cm^{-3}$) | $1.04\times10^{18}$ | $1.04\times10^{18}$ | $1.04\times10^{18}$ |
| Permittivity (F/m) | 11.9 | 11.9 | 11.9 |
| Affinity | 4.05 | 4.05 | 4.05 |

Spectral albedo is a wavelength-specific measure of the amount of diffuse light reflected from the environment. It is an important parameter for bifacial applications [11]–[13]. The spectral albedo of various real-world environments [14] were considered, and the crossed structure was found to perform well in each environment.

## II. DEVICE SIMULATION AND PARAMETER CALIBRATION

This study uses the Silvaco TCAD tool with ray tracing to simulate device performance. The solar cell is operated under a global standard solar spectrum (AM 1.5G) and the light intensity was calculated at wavelengths from 0.3 μm to 1.2 μm with a total incident power density of 100mW/$cm^2$.

For simulation reliability, all parameters were obtained by an initial calibration based on measurement. Since our new devices are based on PERC cells, we use a popular reference [15] for calibration. The models, assumptions and their related parameters were carefully adjusted to minimize the differences to the reported values. Fig. 2 compares the resulting simulated *I-V* curve to the measured result of the PERC solar cell. The close agreement between the two curves in Fig. 2 validates the simulation. The calibrated parameter values are shown in Table 1 and are used for all of our subsequent simulations.

## III. RESULTS AND DISCUSSION

The symmetrical structure obtains a $J_{sc}$ of 31.92 mA/$cm^2$, a $V_{oc}$ of 0.67 V, a *F.F.* of 57.08 % a $\eta$ of 12.31 %, and an energy boost of 88.78% at 100% albedo. Although the energy boost is high, the $\eta$ is still low. The reason is that the distribution of electron carriers is not uniform, thus decreasing $J_{sc}$ and *F.F.* This effect can be seen in Fig. 3, which explores how alignment between the sides affects the electronic current density. Fig. 3a is the symmetrical case (offset = 0 μm). The distribution is, indeed, very non-uniform. As the offset increases to the point of being fully crossed (1480 μm), the electron current covers much more of the silicon area. Table 2 gives the performance of Fig. 3(a)-(e). The crossed structure does have the best performance. The $J_{sc}$ and *F.F.* gradually increase as the device shifts from symmetrical to crossed.

Fig. 4 shows the electric field directions for the crossed structure. Fig. 4(a)-(d) give the directions of the electric field in the p-n gaps. Fig. 4(e) indicates positions of these four gaps, by locating them within the schematic diagram of the crossed structure. Fig. 4(a)-(d) show that the cross structure has both longitudinal and horizontal electric field components. The longitudinal field can transmit carriers to the opposite side. The horizontal electric field occurs simultaneously with the longitudinal field, and therefore forms a surrounding electric field. This surrounding field

facilitates carrier transmission, thereby causing $J_{sc}$ and *F.F.* to increase.

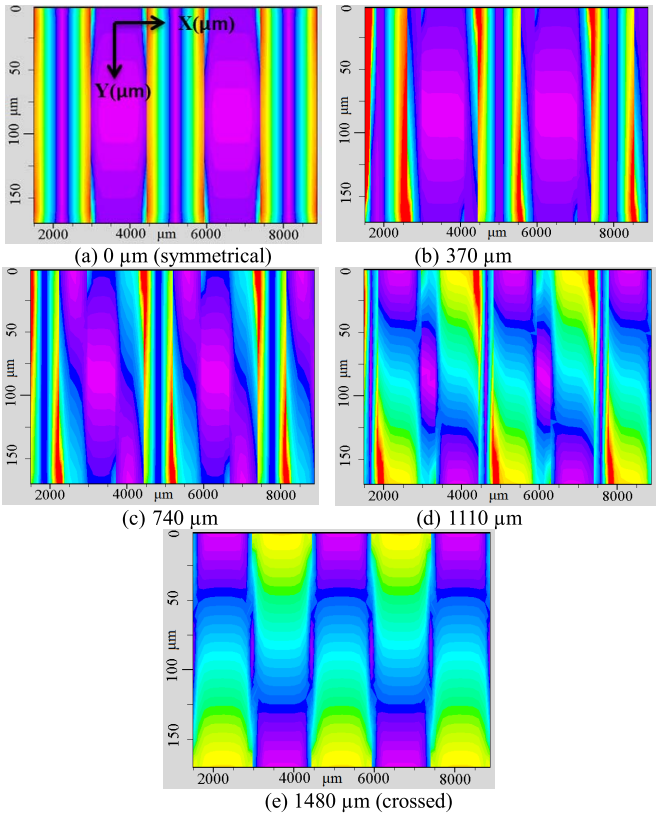


**FIGURE 3.** The electronic current density at various alignment offsets. (a) 0 μm. (b) 370 μm. (c) 740 μm. (d) 1110 μm. (e) 1480 μm. The current density distribution spreads out as the structure becomes more fully crossed.

**TABLE 2.** The performance of Fig. 3 (a)-(e).

| transportations distance | $J_{sc}$ [mA/cm$^2$] | $V_{oc}$ [V] | *F.F.* [%] | η [%] |
|---|---|---|---|---|
| 0 μm (symmetrical) | 31.9 | 0.68 | 57.1 | 12.1 |
| 370 μm | 38.1 | 0.68 | 73.2 | 18.8 |
| 740 μm | 39.4 | 0.67 | 78.6 | 20.9 |
| 1110 μm | 40.0 | 0.67 | 80.9 | 21.8 |
| 1480 μm (crossed) | 40.2 | 0.67 | 81.1 | 21.9 |

We choose the crossed structure for optimization, because it has better performance. The front emitter width ($W_{fe}$), front surface field width ($W_{fs}$), rear emitter width ($W_{re}$) and rear surface field ($W_{rs}$) width can all be optimized. Fig. 5 shows the $J_{sc}$, $V_{oc}$, *F.F.* and $\eta$ performances at various $W_{fe}/(W_{fe}+W_{fs})$ and $W_{re}/(W_{re}+W_{rs})$ ratios. The optimal ratios will depend upon the albedo of the expected operational environment. Fig. 5 and 6 consider the cases of top-side-only (monofacial) illumination and equal (bifacial) illumination.

In Fig. 5(a), $J_{sc}$ is higher when the emitter ratio is larger, with the $W_{fe}$ ratio having the larger impact. The $W_{re}$ ratio

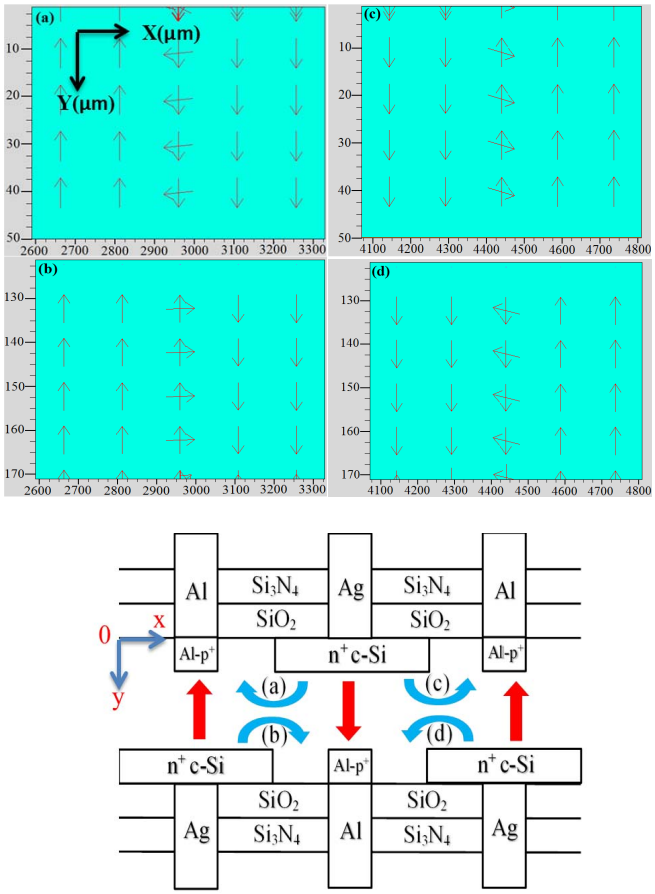


**FIGURE 4.** The electric field of our crossed double-sided passivation emitter and surface field solar cell. (a)-(d) The electric fields in the p-n gaps. (e) Schematic of the electric field in the crossed cell. The crossed placement causes each emitter layer to have a BSF layer across from it, as well as to the left and right. This placement forms a surrounding electric field for minority carriers.

cannot affect $J_{sc}$ when the $W_{fe}$ ratio is above 60% and $J_{sc}$ can reach 40.33 mA/cm$^2$ when the $W_{fe}$ ratio is above 75%. Fig. 5(b) shows that $V_{oc}$ is higher when the ratios are lower. The impact of $W_{fe}$ and $W_{re}$ is similar so the diagram is roughly symmetrical. $V_{oc}$ reaches 0.6775V when the $W_{fe}$ and $W_{re}$ ratios are both 20%. In Fig. 5(c), *F.F.* is higher at lower ratios, with $W_{fe}$ having the larger impact. When the $W_{fe}$ ratio is less than 40%, $W_{re}$ cannot significantly affect *F.F.*, which reaches 81.25% at a $W_{fe}$ ratio of 30%. The power conversion efficiency can reach 21.97% when $W_{fe}$ and $W_{re}$ ratios are 30% and 60% respectively.

Fig. 6 considers the case of bifacial illumination, which means an ideal albedo. Albedo is the measure of the diffuse reflection of solar radiation out of the total solar radiation received by an astronomical body. Comparing these diagrams to their corresponding diagrams in Fig. 5, reveals that the trends are the same: $J_{sc}$ is still higher when the ratios are larger, while $V_{oc}$ and *F.F.* are still higher when the ratios are lower, and $\eta$ is still higher in the middle. The notable difference to Fig. 5 is that the diagrams are fully symmetrical,

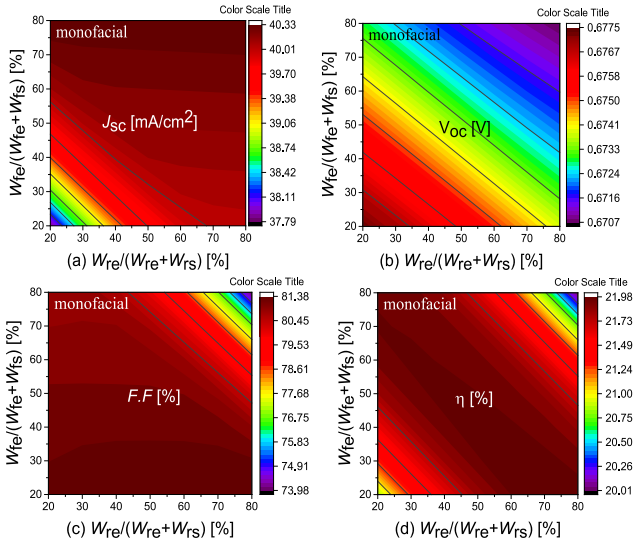


**FIGURE 5.** The influence of $W_{fe}/(W_{fe}+W_{fs})$ and $W_{re}/(W_{re}+W_{rs})$ ratios on the $J_{sc}$, $V_{oc}$, F.F. and $\eta$. (a) the $J_{sc}$ value increases with the increase of emitter ratio. (b)-(c) the $V_{oc}$ and *F.F.* values increase with the decrease of emitter ratio. (d) the highest $\eta$ value is in the middle of the diagram.

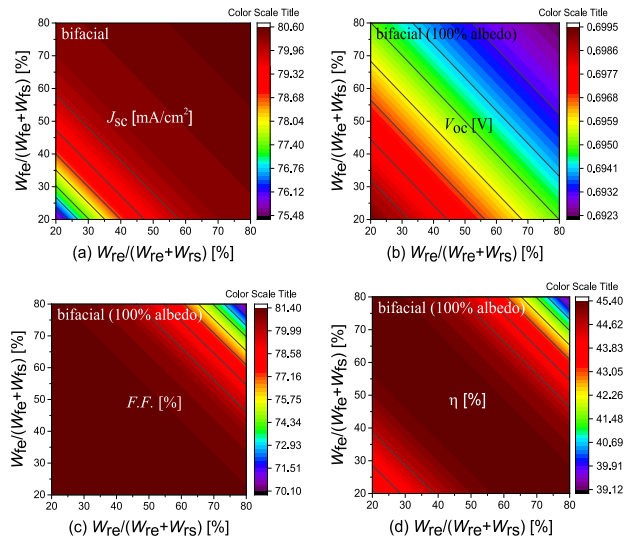


**FIGURE 6.** The influence of $W_{fe}/(W_{fe}+W_{fs})$ and $W_{re}/(W_{re}+W_{rs})$ ratios to the $J_{sc}$, $V_{oc}$, F.F. and $\eta$ for bifacial (100% albedo). (a) (a) the $J_{sc}$ value increases with the increase of emitter ratio. (b)-(c) the $V_{oc}$ and F.F. values increase with the decrease of emitter ratio. (d) the highest $\eta$ value is in the middle of the diagram.

but this is the expected consequence of the two sides being equally important. As for the optimal values, $J_{sc}$ reaches 80.59 mA/cm$^2$ when the $W_{fe}$ and $W_{re}$ ratios are both 80%, $V_{oc}$ reaches 0.6995 V when $W_{fe}$ and $W_{re}$ ratio are both 20%, *F.F.* reaches 81.2 % when the ratios are 20 %, and $\eta$ reaches 45.4% in the middle of Fig. 6(d). Compared with the monofacial case, the bifacial operating environment also has a wider design window.

In typical sunlight, the Shockley–Queisser (SQ) limit of maximum solar conversion efficiency for a single p-n junction photovoltaic cell is around 34 % in theory and 32 % for a silicon-based cell [16]. (Actual cells cannot obtain this limit, due to practical concerns such as front-surface reflection and light blockage from the thin wires on the cell surface.) When considering a bifacial cell operating at 100% albedo, the *effective* power conversion efficiency might be larger than the SQ limit. For example, in this work it is 45.4 % for our newly presented crossed bifacial PERC solar cell. This exceeding of the SQ limit arises from the way that power conversion efficiency is traditionally calculated: only counting front side solar illumination in the denominator (thus ignoring the reflected light entering into the other side of the cell). If that reflected light were also to be considered in the denominator of the limit, then this alternative calculation of conversion efficiency would drop from the reported 45.4 % to a value below the theoretical SQ limit.

**TABLE 3.** The $\eta_{front}$, $\eta_{rear}$ and $\varphi_\eta$ of the symmetrical structure, crossed structure, PERC+ solar cells [7], [9].

| Solar Cell | $\eta$ [%] front/rear | Bifaciality Factor ($\varphi_\eta$) |
|---|---|---|
| ISFH PERC+ [7] | 21.5/16.7 | 0.77 |
| Big Sun PERC+ [9] | 20.7/13.9 | 0.67 |
| LONGi Solar PERC+ [9] | 21.6/17.3 | 0.80 |
| Symmetrical | 12.31/12.31 | 1 |
| Crossed | 21.95/21.95 | 1 |

In Table 3, we compared front side power conversion efficiency ($\eta_{front}$), rear side power conversion efficiency ($\eta_{rear}$) and bifaciality factor ($\varphi_\eta$) of the symmetrical, the crossed and PERC+ solar cells [7], [9]. Because the front of our structure is similar to the rear, the $\eta_{front}$ is the same as the $\eta_{rear}$, and the $\varphi_\eta$ can reach 1. The $\eta_{front}$ and $\eta_{rear}$ of the crossed structure are 0.35% and 4.65% higher, respectively, than the best PERC+ [9]. The gap between $\eta_{front}$ and $\eta_{rear}$ is consequently also reduced.

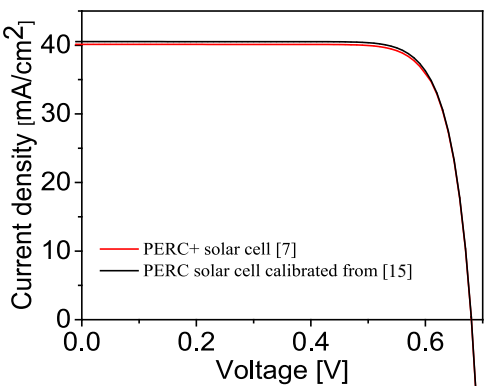


**FIGURE 7.** The *I-V* curves between the conventional PERC solar cell and PERC+ solar cell. The conventional PERC solar cell has better short-circuit current density than the PERC+ solar cell because more light is reflected from the metal layer since it fully covers the rear side.

Fig. 7 shows the *I-V* curves for the conventional standard PERC solar cell (mono-facial) [15] and the PERC+ solar cell (bi-facial) [7]. The conventional PERC cell had already been

calibrated by Silvaco Atlas from the measurement in [15]. A conventional PERC solar cell has the rear-side fully covered by a metal layer. As the figure shows, this improves circuit current density when the albedo is 0 %, because the metal allows for nearly-full reflection of light from the back surface, with no disadvantage from not allowing light in from the rear.

Table 4 shows the benchmark comparisons of the symmetrical structure, crossed structure and PERC+ solar cell under 0% albedo, 30% albedo and 100% albedo. A 0% albedo represents the mono-facial case, a 30% albedo means the average of the spectral albedo of the environment [17], and a 100 % albedo represents the bi-facial case of an ideal environment. Although the symmetric structure's energy boost (Fig. 1(a)) is better than the PERC+ [7], the monofacial operational conversion efficiency is too low. The improved cross structure has good power conversion efficiency in monofacial operation and high-energy boost in bifacial operation. In our previous work, a double-sided symmetrical emitter crystalline silicon solar cell with heterojunction (SHJ) [18], has a high power conversion efficiency and energy boost for bifacial operation that are similar to this present paper. But the crossed structure proposed in this paper can be manufactured by the industry-typical PERC process flow, which has a lower cost and higher market share than SHJ solar cell [8].

**TABLE 4. The comparison of the symmetrical structure, crossed structure, PERC+ solar cell and SHJ solar cell.**

| Solar Cell | Spectral Albedo | $J_{sc}$ [mA/cm$^2$] | $V_{oc}$ [V] | *F.F.* [%] | η [%] | Energy boost [%] |
|---|---|---|---|---|---|---|
| Symmetrical (Fig. 1(a)) | 0 | 31.9 | 0.67 | 57.1 | 12.3 | 0 |
| | 30 | 40.2 | 0.68 | 57.2 | 15.7 | 27 |
| | 100 | 58.0 | 0.69 | 57.5 | 23.2 | 89 |
| Crossed (Fig. 1(b)) | 0 | 40.1 | 0.67 | 81.2 | 22.0 | 0 |
| | 30 | 52.2 | 0.68 | 81.2 | 28.9 | 32 |
| | 100 | 80.3 | 0.69 | 81.3 | 45.4 | 107 |
| PERC+ [7] | 0 | 40.4 | 0.67 | 80.3 | 22.0 | 0 |
| | 30 | 48.9 | 0.68 | 80.4 | 27.0 | 23 |
| | 100 | 68.7 | 0.69 | 80.6 | 38.6 | 75 |
| SHJ [18] | 0 | 36.7 | 0.75 | 83.3 | 22.8 | 0 |
| | 30 | 47.4 | 0.75 | 83.1 | 29.7 | 31 |
| | 100 | 71.5 | 0.77 | 82.9 | 45.5 | 100 |

To explore the impact of our structures under various spectral albedos. Fig. 8 shows the energy boosts of the PERC+ solar cell and the symmetrical and crossed structures, at various spectral albedos. The energy boost of the symmetrical structure and the crossed structure are higher than the PERC+ solar cell. The energy boost of the crossed structure is the largest one at all spectral albedo levels, so it is suitable for bifacial applications.

Fig. 9 shows the crossed structure performance at the spectral albedos of several widely used environments [12]. In the case of snow, these energy boost and $\eta$ values are 100% and 46.4%, respectively, which approaches the performance at ideal albedo. The energy boost is 77.13% for white sand and 20%∼30% under other widely used environments. The results indicate good performance over many environments.

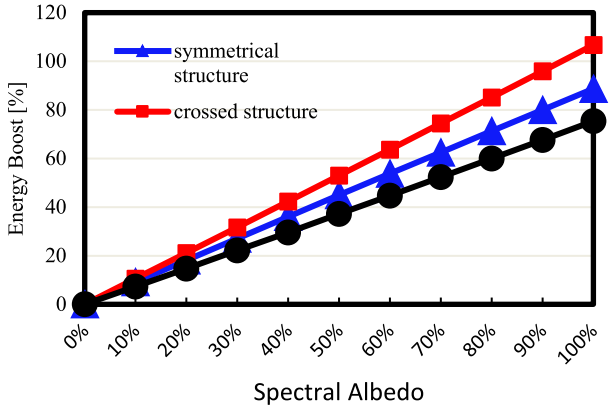


**FIGURE 8. The energy boosts of the PERC+ solar cell, the symmetrical and the crossed structure, for different spectral albedos. The crossed structure has the best energy boost at each spectral albedo.**

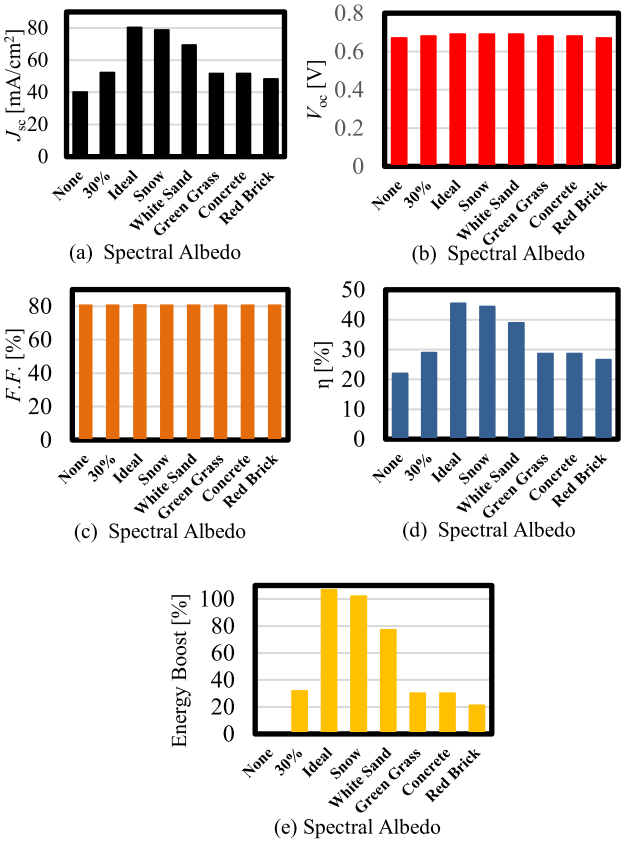


**FIGURE 9. The crossed structure performance under the spectral albedos of several widely used environments. (a) $J_{sc}$ is significantly affected by the environment. (b)-(c) $V_{os}$ and F.F. do not changed significantly across environments. (d) $\eta$ is primarily affected by Jsc. (e) In the case of snow, the energy boost of the crossed structure is 102.06 % which approaches ideal albedo. The crossed structure energy boost can achieve 77.13% in white sand and 20%∼30% under other widely used environments.**

## IV. CONCLUSION

We have designed symmetrical and crossed double-sided passivation emitter and surface field solar cells for bifacial applications, based on PERC solar cell. The crossed

structure has the higher energy boost of the two and is also higher than the conventional PERC+ cell (which suffered from low rear-side power conversion efficiency). Compared to our previous work [18], the crossed structure has similar power conversion efficiency and higher energy boost, but is cheaper to fabricate, it is fully compatible with the PERC fabrication process.

Through the discussion of electronic current density and the electric field, we have evaluated why the crossed structure has better performance. The reason is found to be that the surrounding electric field can significantly improve $J_{sc}$ and *F.F.* We have optimized the crossed structure and found that the best power conversion efficiency occurs at a $W_{fe}$ ratio of 20-50% and a $W_{re}$ ratio of 60-80%. The device exhibits a much better design window for bifacial applications. We therefore consider that our structure can be applied in many lighting environments.

## REFERENCES

[1] K. Yoshikawa *et al.*, "Solar energy materials and solar cells exceeding conversion efficiency of 26% by heterojunction interdigitated back contact solar cell with thin film Si technology," *Solar Energy Mater. Solar Cells*, vol. 173, pp. 37–42, Apr. 2017.
[2] M. J. Kerr, A. Cuevas, and P. Campbell, "Limiting efficiency of crystalline silicon solar cells due to Coulomb-enhanced Auger recombination," *Progr. Photovoltaics Res. Appl.*, vol. 11, no. 2, pp. 97–104, 2003.
[3] A. Richter, M. Hermle, and S. Glunz, "Crystalline silicon solar cells reassessment of the limiting efficiency for crystalline silicon solar cells," *IEEE J. Photovoltaics*, vol. 3, no. 4, pp. 1184–1191, Oct. 2013.
[4] R. Kopecek *et al.*, "Bifaciality: One small step for technology, one giant leap for kWh cost reduction," *Photovoltaics Int.*, vol. 26, pp. 32–45, Jan. 2015.
[5] L. Yalçin and R. Öztürk, "Performance comparison of c-Si, mc-Si and a-Si thin film PV by PVsyst simulation," *J. Optoelectron. Adv. Mater.*, vol. 15, nos. 3–4, pp. 326–334, 2013.
[6] M. Hiroshi, "Radiation energy transducing device," U.S. Patent 3 278 811 A, Oct. 11, 1966.
[7] T. Dullweber *et al.*, "The PERC+ cell: A 21%-efficient industrial bifacial PERC solar cell," in *Proc. 31st Eur. Photovoltaic Solar Energy Conf. Exhibit.*, 2016, pp. 2892–2897, doi: 10.4229/EUPVSEC20152015-2BO.4.3.
[8] *Results 2017 Including Maturity Report 2018*, 9th ed., Int. Technol. Roadmap Photovolt., Frankfurt, Germany, Sep. 2018.
[9] T. Dullweber *et al.*, "Bifacial PERC+ solar cells: Status of industrial implementation and future perspectives," in *Proc. BIFI Workshop*, 2017, pp. 1–39.
[10] J. Zhao, A. Wang, and M. A. Green, "Emitter design for high-efficiency silicon solar cells. Part I: Terrestrial cells," *Progr. Photovoltaics Res. Appl.*, vol. 1, no. 3, pp. 193–202, 1993.
[11] R. W. Andrews and J. M. Pearce, "The effect of spectral albedo on amorphous silicon and crystalline silicon solar photovoltaic device performance," *Solar Energy*, vol. 91, pp. 233–241, May 2013.
[12] M. P. Brennan, A. L. Abramase, R. W. Andrews, and J. M. Pearce, "Effects of spectral albedo on solar photovoltaic devices," *Solar Energy Mater. Solar Cells*, vol. 124, pp. 111–116, May 2014.
[13] B. Soria, E. Gerritsen, P. Lefillastre, and J.-E. Broquin, "A study of the annual performance of bifacial photovoltaic modules in the case of vertical facade integration," *Energy Sci. Eng.*, vol. 4, no. 1, pp. 52–68, 2016.
[14] T. C. R. Russell, R. Saive, A. Augusto, S. G. Bowden, and H. A. Atwater, "The influence of spectral albedo on bifacial solar cells: A theoretical and experimental study," *IEEE J. Photovoltaics*, vol. 7, no. 6, pp. 1611–1618, Nov. 2017.
[15] F. Ye *et al.*, "22.13% Efficient industrial p-type mono PERC solar cell," in *Proc. Conf. Rec. IEEE Photovoltaic Spec. Conf.*, 2016, pp. 3360–3365.
[16] S. Rühle, "Tabulated values of the Shockley–Queisser limit for single junction solar cells," *Solar Energy*, vol. 130, pp. 139–147, Jun. 2016, doi: 10.1016/j.solener.2016.02.015.
[17] X. Sun, M. R. Khan, C. Deline, and M. A. Alam, "Optimization and performance of bifacial solar modules: A global perspective," *Appl. Energy*, vol. 212, pp. 1601–1610, Feb. 2018.
[18] J.-T. Lin *et al.*, "Double-sided symmetrical and crossed emitter crystalline silicon solar cells with heterojunctions for bifacial applications," *IEEE J. Photovoltaics*, vol. 8, no. 2, pp. 441–447, Mar. 2018.

**JYI-TSONG LIN** (M'96–SM'08) was born in Taiwan, in 1959. He received the B.S. degree in physics from National Taiwan Normal University, Taipei, Taiwan, in 1982, the M.S. degree in electronics from National Chiao Tung University, Hsinchu, Taiwan, in 1984, and the Ph.D. degree in electronics and computer science from the University of Southampton, Southampton, U.K., in 1993. He has been with the National Sun Yat-Sen University, Kaohsiung, Taiwan, since 1984, where he is currently a Professor with the Department of Electrical Engineering. His research interests include the design and modeling of small-geometry SOI devices and the design of high-speed and low-power circuits of bulk and SOI MOSFETs. He was recently working on the development and process integration of nonclassical SOI, TFT nanodevices, TFET, solar cell, and one transistor memory.

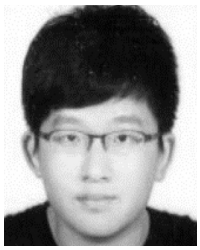

**KON-YU HO** received the M.S. degree in electrical engineering from National Sun Yat-sen University, Kaohsiung, Taiwan. His current research interests include bifacial solar cells and nano TFETs.

**STEVE W. HAGA** received the Ph.D. degree in electrical engineering from the University of Maryland, College Park, MD, USA. He is currently an Assistant Professor with the Department of Computer Science and Engineering, National Sun Yat-sen University, Kaohsiung, Taiwan. His current research interests include compiler optimizations for real-time systems and GPGPUs, computer architectures, and memory systems.

**WEN-HAO CHEN** received the M.S. degree in electrical engineering from National Sun Yat-sen University, Kaohsiung, Taiwan. His current research interests include bifacial solar cells and nano devices.